



ELF waves generated by modulated HF heating of the auroral electrojet and observed at a ground distance of ~ 4400 km

R. C. Moore,^{1,2} U. S. Inan,¹ T. F. Bell,¹ and E. J. Kennedy³

Received 8 September 2006; revised 21 December 2006; accepted 19 January 2007; published 22 May 2007.

[1] We present calibrated measurements of ELF waves generated by modulated HF heating of the auroral electrojet by the High frequency Active Auroral Research Program (HAARP) HF transmitter in Gakona, Alaska, and detected after propagating more than 4400 km in the Earth-ionosphere waveguide to Midway Atoll. The magnitude of the 2125 Hz wave received at Midway Atoll is consistent with the radiation from a horizontal dipole located at the altitude of the maximum Hall conductivity variation (created by modulated HF heating) and radiating $\sim 4\text{--}32$ W. The HF-ELF conversion efficiency at HAARP is thus estimated to be $\sim 0.0004\text{--}0.0032\%$ for the 2125 Hz wave generated using sinusoidal amplitude modulation.

Citation: Moore, R. C., U. S. Inan, T. F. Bell, and E. J. Kennedy (2007), ELF waves generated by modulated HF heating of the auroral electrojet and observed at a ground distance of ~ 4400 km, *J. Geophys. Res.*, 112, A05309, doi:10.1029/2006JA012063.

1. Introduction

[2] Modulated heating of the ionosphere in the presence of high-altitude, naturally forming electric currents, such as the auroral electrojet and midlatitude dynamo currents, has been investigated as a means for the generation of electromagnetic waves in the extremely low frequency (ELF, 3–3000 Hz) band since the 1970s [e.g., *Getmantsev et al.*, 1974; *Stubbe et al.*, 1982; *Ferraro et al.*, 1982; *Lunnen et al.*, 1984; *Barr et al.*, 1991; *Vilaseñor et al.*, 1996; *Moore et al.*, 2006]. The coupling of ELF signals generated in this manner to the Earth-ionosphere waveguide, in which ELF signals can propagate to large distances with relatively low attenuation, is important in the context of assessing the potential use of such a system for long-distance communications.

[3] Long-distance detection of ELF waves generated by modulated HF heating of natural, large-scale current systems has been attempted on several occasions. *Ferraro et al.* [1982] presented results indicating the detection in Pennsylvania of a 2073 Hz signal generated by the Tromsø heater in Norway, ~ 6000 km distant. The results of this experiment have been repeatedly called into question by *Barr et al.* [1986, 1991] and *Barr* [1998], whose calculations indicate that the ELF signal strengths should have been well below detectable ranges. *Lunnen et al.* [1984] presented the detection in Puerto Rico of a

2500 Hz signal generated by the Jicamarca radar in Peru, ~ 3500 km distant. However, as noted by *Barr et al.* [1991], the signal of interest was not shown to be significantly above the noise floor. Currently, the most reliable set of experimental results in regard to the long-distance detection of ELF signals generated in this manner and propagating in the Earth-ionosphere waveguide has been provided in studies by *Barr et al.* [1985, 1986, 1991], each of which presents calibrated measurements of ELF waves generated using the Tromsø HF heating facility. *Barr et al.* [1985] found that a ~ 1 W ELF transmission at the altitude of the maximum Hall conductivity variation (created by modulated HF heating) was consistent with observations in the 1000–1500 Hz band using measurements at receivers located 17, 205, and 554 km from the transmitter. *Barr et al.* [1986] expanded the measurements to the 500–5500 Hz band and analyzed the polarization of the received signal, showing that observations closely matched the polarizations predicted by accounting for the propagation effects within the Earth-ionosphere waveguide. *Barr et al.* [1991] presented ELF measurements detected 2050 km from the HF transmitter with signal-to-noise ratio (SNR) levels >10 dB using 20 min long integration periods at modulation frequencies of 3010 and 6020 Hz. The polarization of the received wave as a function of ELF frequency was used to select appropriate Earth-ionosphere waveguide parameters to describe the propagation. While long-distance measurements of ELF signals generated by modulated HF heating of the large-scale current systems have been presented using the HF ionospheric research facilities at Tromsø and Jicamarca, no such long-distance measurements have yet been presented for ELF waves generated using the high-power HF transmitter at the High frequency Active Auroral Research Program (HAARP) research station in Gakona, Alaska. The HAARP HF transmitter (or heater), which

¹Department of Electrical Engineering, Stanford University, Stanford, California, USA.

²Now at Department of Electrical and Computer Engineering, University of Florida, Gainesville, Florida, USA.

³Information Technology Division, U.S. Naval Research Laboratory, Washington, DC, USA.

operates at similar power levels and frequencies as the Tromsø heater, is the principle component in a suite of instruments at the facility through which experiments in ionospheric physics are conducted.

[4] In this paper we present conclusive evidence of the detection of ELF signals generated by modulated HF heating of the auroral electrojet by the HAARP HF transmitter at a ground distance of 4461 km at Midway Atoll, more than twice the distance from the HF transmitter than that presented by *Barr et al.* [1991]. The polarization of the observed ELF signal at 2125 Hz is used to identify a range of possible ionospheric parameters, and the magnitude of the observed ELF wave is used to estimate the power radiated at 2125 Hz in the context of a realistic Earth-ionosphere waveguide propagation model.

2. Instrumentation

[5] The data presented in this paper were acquired using Stanford University ELF/VLF receivers located in Chistochina, Alaska (~ 36 km from the HAARP facility at 62.61°N , 144.62°W), and at Midway Atoll (~ 4461 km from the HAARP facility at 28.21°N , 177.38°W). Each receiver utilizes two orthogonal air-core loop antennas oriented to detect the horizontal components of the wave magnetic field on the ground, a preamplifier located near the antennas, and a line receiver and data-recording system located ~ 600 m from the antennas in order to reduce the effects of electromagnetic noise associated with 60 Hz hum and its harmonics. Both receiver channel inputs have radio frequency interference (RFI) suppression units to reduce interference from differential signals at frequencies above 100 kHz, including the HF band. The analog receiver channel outputs are antialias filtered at 40 kHz (using an eight-pole Chebyshev filter) and sampled with 16 bit resolution at 100 kHz. The timing trigger used with the analog-to-digital converter has an absolute timing error < 150 ns, and the frequency of the trigger is accurate to three parts in 10^{-12} . Thus the timing accuracy of the analog-to-digital conversion easily supports the hour-long integration periods used in this paper for the detection of coherent signals.

[6] The Stanford University ELF/VLF receiver equipment used at Chistochina and at Midway Atoll has been rigorously tested in order to establish that the ELF/VLF signals received were not artificially created in the receivers by nonlinear demodulation of the HF sky wave arriving at the site. Two possible electronic couplings are of particular interest: coupling via common mode signals and coupling via differential mode signals. While common mode signals at 1.6 MHz were reduced by 40 dB compared to signals at 1 kHz, common mode signals at higher frequencies were too small to be measured. Additionally, differential mode signals measured at 1 MHz were reduced by 40 dB from the 1 kHz value. Higher-frequency, differential mode signals were also too small to measure accurately.

[7] Over the course of the 4 hour experiment, no other potential sources for the observed ELF signals were in operation near the receiver systems at Midway Atoll and Chistochina. Together, these considerations strongly suggest that the ELF/VLF signals observed at each ELF/VLF

receiver are indeed generated by modulated heating of the auroral electrojet currents.

3. Description of the Experiment

[8] The experiment reported in this paper was conducted at the HAARP facility between 0800 and 1200 UT on 11 February 2005 under nighttime ionospheric conditions. The HAARP HF transmitter operated at 3.25 MHz with X-mode polarization during hour-long sinusoidal amplitude modulation periods, alternating each hour between modulation frequencies of 575 and 2125 Hz. The HF beam was directed vertically for all transmissions, and the input HF power was 960 kW during the experiments to be described, similar to the 1.08 MW used during the Tromsø experiments [*Barr and Stubbe*, 1991]. Geomagnetic conditions varied over the 4 hour transmission period: The 0600–0900 UT period is characterized by a Kp index of 2^+ , while the 0900–1200 UT period is characterized by a Kp index of 3^+ . The subsequent 3 hour period saw a return of the Kp index to a value of 2^+ . During the first 3 hours of the experiment the absolute value of all components of the fluxgate magnetometer located at the HAARP facility remained less than 50 nT, while the last hour of the experiment saw the absolute value of the fluxgate magnetometer data fluctuate above 300 nT.

4. Experimental Data

[9] Measurements made near HAARP (at Chistochina, see Figure 1) are used for the comparison of this experiment with previous long-distance ELF detection experiments, while distant measurements (at Midway Atoll, see Figure 1) are used to assess the level of ELF energy successfully injected into the Earth-ionosphere waveguide. In this section we will present the measurements made near HAARP followed by observations in the distant far field.

4.1. Measurements at Chistochina

[10] Depending on the frequency of the ELF wave generated, observations at Chistochina may be considered to be in either the near field or the far field. Assuming a horizontal dipole source at altitude h above a ground plane (and HAARP), it can be shown that the amplitude of the B field measured at Chistochina is a function of the signal wavelength λ and the total distance r between the dipole and the receiver:

$$|B| \propto \frac{h}{r^3} \sqrt{1 + \left(\frac{2\pi r}{\lambda}\right)^2}, \quad (1)$$

where $r = \sqrt{h^2 + d^2}$ and d is the ground distance between HAARP and Chistochina. From equation (1) it is apparent that at small distances (i.e., in the near field) the signal amplitude varies as $1/r^3$, while at larger distances (i.e., in the far field) the signal amplitude varies as $1/r^2$. *Barr et al.* [1986] showed that an effective Hall modulation dipole at ~ 70 – 80 km altitude accurately modeled observations of the ELF/VLF signal polarization in the far field. For an effective Hall modulation dipole altitude of $h = \sim 75$ km, equation (1) may be used to show that at 575 Hz the B-field amplitude at Chistochina consists of approximately equal parts

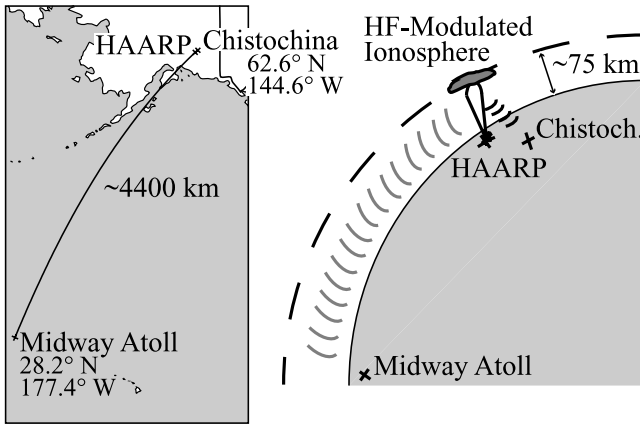


Figure 1. Geometry of the experiment.

of near-field and far-field components, while at 2125 Hz the far-field component dominates by a factor of ~ 10 .

[11] The magnitude of the ELF fields received at Chistochina over the 4 hour transmission period are shown as a function of modulation frequency and time in Figure 2. In general, the strength of ELF wave generation is in the same range as previous observations in Alaska [e.g., Kimura *et al.*, 1991; Papadopoulos *et al.*, 2005; Platino *et al.*, 2006], although during the 1100–1200 UT hour the 2125 Hz signal reaches a magnitude of 70 dB fT, ~ 10 dB stronger than the 1570 Hz signal detected 17 km from Tromsø by Barr *et al.* [1985]. Signal magnitudes of 70 dB fT are also ~ 10 dB stronger than the measurements (also at Chistochina) reported by Platino *et al.* [2006], who used satellite observations of ELF signals at frequencies < 1 kHz to approximate a radiated power level of ~ 1 –4 W from the HAARP-heated ELF source region. A simple estimate based on these observations indicates that the far-field ELF source dipole during the 1100–1200 UT hour can be expected to be ~ 10 dB stronger than the 1 W estimated by Barr *et al.* [1985] or the 1–4 W estimated by Platino *et al.* [2006], i.e., on the order of 10 W.

[12] The variation of the observed signal magnitudes at Chistochina may also help interpret observations at Midway Atoll. While the magnitude of the 2125 Hz signal observed at Chistochina during the 1100–1200 UT hour is ~ 10 dB higher than the magnitude during the 0900–1000 UT hour, the magnitude of the received 575 Hz signal during the 0800–0900 UT hour is approximately equal to that observed during the 1000–1100 UT hour. The Gakona flux-gate magnetometer remains relatively quiet throughout the

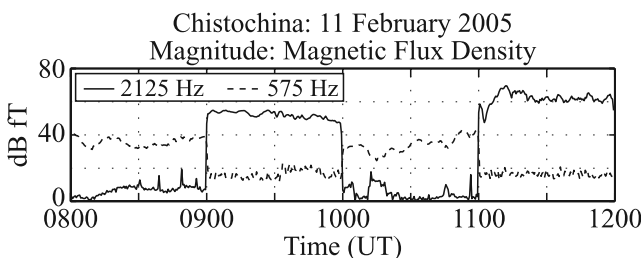


Figure 2. Magnitude of ELF observations at Chistochina at 575 and 2125 Hz as a function of time.

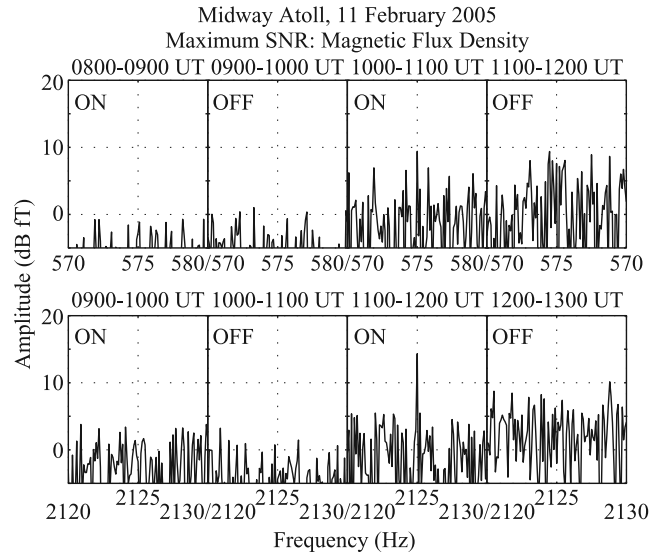


Figure 3. Hour-long discrete Fourier transforms (DFTs) of observations at Midway Atoll: (top) 575 Hz and (bottom) 2125 Hz. The antenna orientation has been rotated in postprocessing to maximize the signal-to-noise ratio. A 10 Hz window is shown in each case for ELF magnitudes calculated every 0.1 Hz.

experiment until several minutes before 1100 UT, at which time the observed signal magnitude increases dramatically and remains high for the next ~ 45 min. The higher magnitude of the 2125 Hz signal during the 1100–1200 UT hour may thus be attributed to the presence of a stronger electrojet current. This stronger electrojet current indicates that far-field measurements at Midway Atoll may be more likely to detect the 2125 Hz signal during the 1100–1200 UT hour than during the 0900–1000 UT hour. However, the attenuation rate of the Earth-ionosphere waveguide between HAARP and Midway Atoll may likely be the dominant factor in regard to signal detection at Midway Atoll.

4.2. Measurements at Midway Atoll

[13] In the distant far field at Midway Atoll, hour-long discrete Fourier transforms (DFTs) are employed to detect the 575 and 2125 Hz tones. In order to first demonstrate the positive detection of each signal we rotate the antenna orientation in postprocessing to maximize the SNR in a 10 Hz bandwidth centered on each frequency. Because the noise environment is dominated by the impulsive electromagnetic emanations from lightning (sferics), the noise level as a function of antenna direction depends on the location of active thunderstorms at the time of the experiment. Thus the SNR is not necessarily maximized when the antenna is aligned with the maximum magnetic field of the signal (accounting for the signal polarization). Using measurements from our two orthogonal loop antennas, we rotate (in postprocessing) our antennas through 360° in order to find the antenna direction which maximizes the SNR. The results are shown in Figure 3, and the maximum SNR obtained at 575 and 2125 Hz are 2.5 and 8.8 dB, respectively, during the last two hour-long transmissions.

[14] Although neither ELF signal was detected at Midway Atoll during the first 2 hours of transmission, the causal

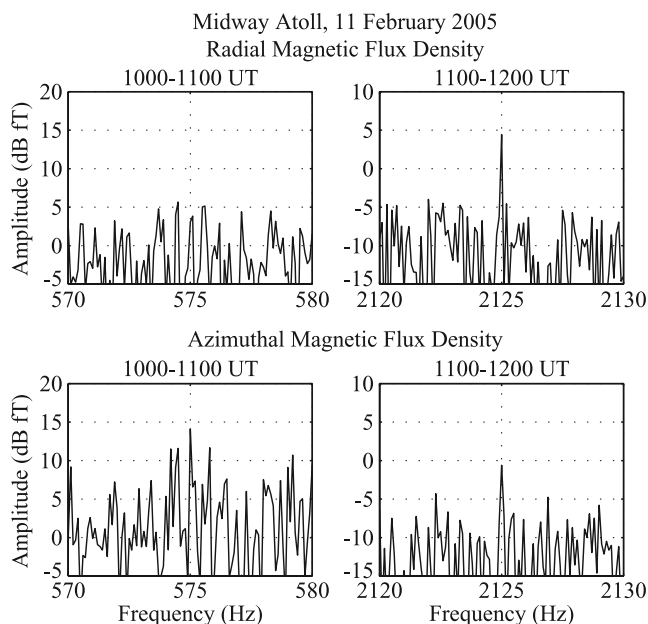


Figure 4. Hour-long DFTs of the radial and azimuthal components of successfully detected ELF signals at Midway Atoll: (left) 575 Hz and (right) 2125 Hz. A 10 Hz window is shown in each case for ELF magnitudes calculated every 0.1 Hz.

relationship between the observations and the transmission schedule during the second transmission at each frequency is apparent: The signal of interest disappears during the respective off periods. Although the noise level in the 10 Hz band surrounding 575 Hz is observed to increase during the final hour, the 575 Hz signal is still 1.8 dB larger during the on period than during the subsequent off period. This fact, coupled with the 2.5 dB SNR observed during the on period, indicates that the 575 Hz signal is positively detected. The fact that the 2125 Hz signal was detected during the 1100–1200 UT hour and not during the 0900–1000 UT hour is not entirely unexpected, considering the ~ 10 dB difference in Chistochina observations during these hours. On the other hand, the fact that the 575 Hz signal is detected at Midway Atoll during the 1000–1100 UT hour and not during the 0800–0900 UT hour suggests a higher waveguide attenuation rate during the 0800–0900 UT hour than during the 1000–1100 UT hour.

[15] Having established the successful detection of each signal at Midway Atoll during the last 2 hours of transmission, we now analyze the radial and azimuthal components of each received signal, where the radial component is the portion of the signal parallel to the great circle path and the azimuthal component is the portion of the signal perpendicular to the great circle path. Figure 4 shows the radial and azimuthal components (using a 1 hour integration period) of the positively detected ELF fields at each frequency during their respective transmission hours. While the azimuthal component of the 575 Hz signal is ~ 2.5 dB above the largest noise component in the 10 Hz band, the radial component is at least 10 dB smaller than the azimuthal component and also within the noise floor, precluding detailed polarization measurements. The fact that the azi-

muthal component of the 575 Hz signal is at least 10 dB larger than the radial component is consistent with previous observations by *Barr et al.* [1986] and previous theoretical analyses by *Barr et al.* [1991] near that frequency.

[16] While the 575 Hz measurements are not ideal for polarization calculations, at 2125 Hz both the radial and the azimuthal components are detected during the 1100 UT hour with $\text{SNR} > 3$ dB. It is readily apparent from Figure 4 that the radial component of the magnetic field is significantly stronger than the azimuthal component, a relationship opposite that observed at 575 Hz. This observation is consistent with previous observations by *Barr et al.* [1986] and is consistent with the fact that the cutoff frequency for the first quasi-transverse electric (QTE) waveguide mode is between 575 and 2125 Hz. The fact that the relative levels of the radial and azimuthal components of the received field reveal waveguide characteristics, such as the range of the first QTE cutoff frequency, has been employed by *Barr et al.* [1986, 1991] to identify reasonable ionospheric electron density variations with altitude which yield wave polarizations that match observations.

[17] The polarization of the received ELF signals is independent of the strength and excitation phase of the ELF source dipole and will be used herein to approximately characterize ionospheric propagation parameters. To be consistent with the previous work of *Barr et al.* [1986], the polarization is here defined as

$$P = \frac{B_r}{B_a} = |P| \exp(j\angle P), \quad (2)$$

where B_r and B_a are the complex valued radial and azimuthal components of the magnetic flux density, respectively. The polarization and magnitude of the received signals are summarized in Table 1, where the error range has been approximated by incorporating the observed average noise level in the 10 Hz band.

5. Analysis

[18] The numerical analysis performed in this section relies on two separate physical models: one model to calculate ELF wave propagation in the Earth-ionosphere waveguide and one model to calculate the altitude of the Hall current maximum during the HF heating process. In order to approximate the ELF energy coupling to the Earth-ionosphere waveguide we employ the long-wave propagation capability (LWPC) code [*Pappert and Snyder, 1972; Pappert and Morfitt, 1975; Ferguson and Snyder, 1987*], a multiple-mode model that uses realistic parameters for the ground conductivity, the Earth's magnetic field, and the altitude profile of nighttime ionospheric conductivity. LWPC is a two-dimensional (2-D) code which accounts for coupling between waveguide modes and necessarily assumes ionospheric homogeneity in the dimension transverse to the direction of propagation [*Pappert and Snyder, 1972; Ferguson and Snyder, 1987*]. Given an altitude and orientation of the radiating dipole, along with the electron density variation with altitude along the path of propagation, LWPC is used to calculate the radial and azimuthal magnetic field components at the receiver. Although LWPC accounts for the boundary conditions imposed by the iono-

Table 1. Summary of Wave Polarization Observations at Midway Atoll: 11 February 2005

Frequency, Hz	$ B $, dB fT	$ P $, dB	$\angle P$, deg
575	14.2 ± 2.0	< -10	N/A
2125	5.5 ± 1.4	5.1 ± 3.0	99 ± 20

spheric plasma and the conductive ground when calculating waveguide excitation factors, LWPC assumes the radiating dipole is operating within the free space portion of the waveguide, rather than within the ionospheric plasma. This assumption necessarily neglects any small amount of attenuation experienced by the ELF signal in the D region ionosphere prior to exciting the waveguide as well as any transmission loss experienced in coupling from the ionosphere to free space. In addition, the polarization of the modeled wave at Midway Atoll is not sensitive to changes in the altitude and orientation of the radiating dipole for the ionospheric parameters used in this paper. The calculated polarization at the receiver thus depends only on the ionospheric electron density profile employed.

[19] While the polarization of the calculated field at the receiver is independent of the altitude and orientation of the radiating dipole, the magnitude of the calculated field depends heavily on the altitude and orientation of the radiating dipole. In this work, as in the work of *Barr et al.* [1991], the radiating dipole is taken to be at the height of the Hall current maximum, and the orientation of the horizontal radiating dipole is taken to be along the geomagnetic east-west direction. For the electron density profiles that are able to support the wave polarizations observed at Midway Atoll the altitude of the Hall current maximum is calculated using an HF heating model similar to that described by *James* [1985] but which accounts for the sinusoidal amplitude modulation used during this experiment. The altitudes of the Hall current maxima were rounded to the nearest 5 km in order to simplify the propagation calculations involving LWPC.

[20] We begin our numerical analysis using a set of ionospheric electron density profiles of the form used by *Wait and Spies* [1964] with $h' = 80$ and 85 km and $\beta = 0.45$ –1.0, and we will later compare these results to those calculated for more realistic ionospheric electron density profiles used in previous publications. Modeling results involving the 575 Hz signal are not very revealing. Virtually all ionospheric electron density profiles employed result in a wave polarization magnitude < -10 dB. The resulting range in radiated power level is thereby rather large, and the only definitive conclusion that can be drawn is that the radiated power from the 575 Hz dipole is less than ~ 1 kW. Similar results were found using the more realistic electron density profiles used later in this section. Because the measurements at 575 Hz are not restrictive enough to be useful for model comparisons, we ignore the 575 Hz signal through the remainder of this analysis.

[21] While the modeling results for the 575 Hz signal do not significantly restrict the range of possible radiated power levels for our idealized dipole above the HAARP HF heater, model results for the 2125 Hz signal are more definitive. The polarization of the modeled 2125 Hz signal

along with the height h_σ and strength P_{rad} of the radiating dipoles are provided in Table 2. The calculated polarizations for this set of ionospheres are well distributed over the range of polarizations observed at Midway Atoll, and the resulting radiated power levels range from ~ 4 to 85 W. Among the profiles listed the $h' = 80$ km and $\beta = 0.80$ profile yields wave polarization parameters that are closest to our average observations and indicates a radiated power level of 9–17 W. A radiated power level in the range of tens of watts is not particularly surprising considering the SNR of our measurements at Midway Atoll and the fact that our measurements near the ELF source region at Chistochina are somewhat stronger than those reported by *Barr et al.* [1985] and *Platino et al.* [2006], who concluded a radiated power on the order of 1 W. On the other hand, 85 W seems rather high, and the exponential ionospheric profiles used here may be considered to be too sharp to represent realistic ionospheric electron density profiles. At the same time, it can be seen from Table 2 that, in general, as the electron density profile sharpens (as β increases), the resulting polarization magnitude decreases and the resulting radiated power level decreases. We will use this observation in the analysis using more realistic ionospheric electron density profiles.

[22] While the exponential profiles used above may be considered too sharp to represent realistic ionospheric profiles, electron density profiles I–VI and VIII–X shown in Figure 5 have been used in previous ionospheric work and are used here to analyze the ELF signals at Midway Atoll. Profiles I–III have been used in VLF propagation studies by *Lev-Tov et al.* [1995] and *Moore et al.* [2003], while profiles III–VI have been used for subauroral work by *Demirkol et al.* [1999]. Profile VII is a linear combination of profiles I, II, and III and was selected as a rough

Table 2. Summary of LWPC Calculations: Exponential Electron Density Profiles^a

h' , km	β	$ P $, dB	$\angle P$, deg	h_σ , km	P_{rad} , W
80	0.45	10.0	81.6		
80	0.50	9.6	92.6		
80	0.55	8.8	97.1		
80	0.60	6.1	103.3	80	45.2–85.1
80	0.65	7.1	102.2	80	34.6–65.1
80	0.70	6.2	103.7	80	20.2–38.1
80	0.75	5.5	99.9	80	12.8–24.2
80	0.80	5.1	98.1	80	9.0–16.9
80	0.85	4.8	96.4	80	9.4–17.7
80	0.90	4.5	94.3	80	5.3–10.0
80	0.95	4.4	92.7	80	4.4–8.3
80	1.00	4.2	90.9	80	3.8–7.2
85	0.45	9.6	84.0		
85	0.50	10.1	89.8		
85	0.55	10.2	96.8		
85	0.60	8.3	113.2		
85	0.65	7.5	120.5		
85	0.70	6.6	121.6		
85	0.75	5.5	122.6		
85	0.80	4.6	121.9		
85	0.85	3.8	118.8	85	25.5–47.9
85	0.90	3.2	115.4	85	15.7–29.6
85	0.95	2.8	112.6	85	10.5–19.8
85	1.00	2.5	109.2	85	7.1–13.4

^aLWPC, long-wave propagation capability.

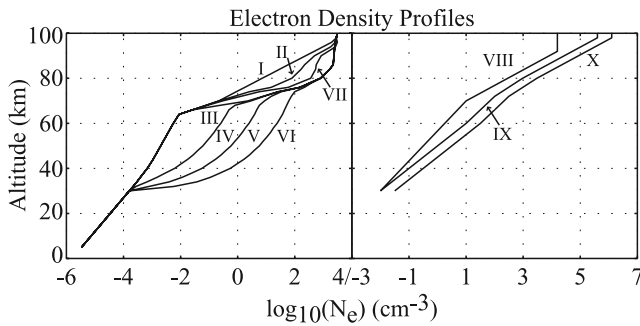


Figure 5. Realistic electron density profiles used to assess the propagation of the 2125 Hz signal to Midway Atoll.

attempt to minimize the magnitude of the modeled field polarization at Midway Atoll. Profiles VIII–X have been approximated from the nighttime ionospheric profiles presented by *Barr et al.* [1986]. The results of the analyses, using these more realistic ionospheric electron density profiles, are summarized in Table 3. It can be seen from Table 3 that profiles II, III, IV, and VII yield polarizations that are within the error range of our observations at Midway Atoll. Although these more realistic profiles do not fully bound the error range of our observations at Midway Atoll, the profiles that yield wave polarizations that are within the error range also yield radiated power levels of 9–32 W. The ionospheric electron density profile that most closely matches the average magnitude of our observed wave polarization yields a radiated power level of 9–17 W, which is the same range found for the exponential profiles previously employed.

[23] While the exponential electron density profiles employed yield radiated power levels of ~ 4 –85 W, the more realistic ionospheric profiles yield a radiated power level ranging from 9 to 32 W. In both cases the electron density profile that yields wave polarization magnitudes closest to the average observed polarization magnitude also indicates a radiated power level of 9–17 W. The more realistic electron density profiles would appear to benefit from a slight sharpening of the profiles, reducing the magnitude of the modeled polarization. Along with a reduction of the modeled polarization magnitude the radiated power would also decrease, rather than increase, as indicated from the analysis of the exponential profiles. It thus appears likely that a more realistic estimate of the power radiated at 2125 Hz would be limited to ~ 32 W. Together, the analyses using exponential profiles and the more realistic profiles indicate a radiated power of ~ 4 –32 W from an altitude of 75–80 km.

[24] The ~ 4 –32 W range of radiated power is also approximately consistent with our observations at Chistochina. Assuming the heated ionospheric region may be approximated by a horizontal electric dipole at altitude h above a perfectly conducting ground, the expression for the radiated power as a function of current moment Idl is [Balanis, 1982]

$$P_{rad} = \eta \frac{\pi}{2} \left| \frac{Idl}{\lambda} \right|^2 \left[\frac{2}{3} - \frac{\sin(2\beta h)}{2\beta h} - \frac{\cos(2\beta h)}{(2\beta h)^2} + \frac{\sin(2\beta h)}{(2\beta h)^3} \right], \quad (3)$$

where β is the wave number and η is the intrinsic impedance of free space. Under the same assumptions the magnitude of the horizontal component of the magnetic flux density at the receiver may be expressed as

$$|B_{horiz}| = \frac{\mu_0 Idlh}{2\pi r^3} \sqrt{1 + (\beta r)^2}, \quad (4)$$

where μ_0 is the permeability of free space and r is the total distance between the dipole and the receiver. Equations (3) and (4) may be combined to show that a dipole radiating ~ 4 –32 W at 2125 Hz from an altitude of 75–80 km produces magnetic flux densities of ~ 63 –72 dB fT at Chistochina. Accounting for a more realistic lossy ground plane using the near-field formulation provided by *Platino et al.* [2006] produces negligible differences from these results. The ~ 63 –72 dB fT range overlaps significantly with the 60–66 dB fT standard error range observed at Chistochina during the 1100–1200 UT hour. It thus appears that the radiated power level of 4–32 W estimated using measurements ~ 4400 km from the HAARP HF transmitter at Midway Atoll is also consistent with observations ~ 36 km from the HAARP facility at Chistochina.

6. Discussion and Summary

[25] We have presented definitive experimental evidence of the detection of ELF signals at 575 and 2125 Hz, generated by modulated HF heating of the auroral electrojet current system, at a ground distance of 4461 km from the ELF source region. A long-wavelength propagation model bounds the radiated power of the 2125 Hz effective dipole to ~ 4 –32 W. The resulting HF-ELF conversion efficiency of ~ 0.0004 – 0.0032% is ~ 10 times larger than those found in previous analyses [e.g., *Barr et al.*, 1985]. However, the ELF amplitudes observed at Chistochina during this experiment were larger than those observed in these previous analyses, indicating that ELF wave generation was simply stronger during our experiment than during the previous analyses. Nevertheless, the attenuation rate of the Earth-ionosphere waveguide may likely be the dominant factor in regard to signal detection in the far field. The positive detection of ELF signals at Midway Atoll, using a 1 hour integration time period during which the ELF source parameters are observed to vary significantly in local magnetometer data, indicates that the auroral electrojet

Table 3. Summary of LWPC Calculations: Realistic Electron Density Profiles

Ionosphere	$ P $, dB	$\angle P$, deg	h_{σ} km	P_{rad} , W
I	10.1	89.9		
II	6.9	79.8	80	6.5–12.3
III	6.4	86.3	75	15.9–29.9
IV	6.9	87.4	75	17.1–32.2
V	8.3	92.0		
VI	14.5	85.6		
VII	4.9	81.2	80	9.1–17.1
VIII	10.8	84.5		
IX	12.9	84.8		
X	15.1	87.7		

may be used as a stable source for ELF wave generation, even under variable ionospheric conditions and can be used to perform long-distance studies of the coupling of ELF energy to the Earth-ionosphere waveguide.

[26] At distances as large as 4400 km we are significantly limited in our analysis by a relatively weak SNR. In this regard, nonlinear signal detection methods, such as the data-clipping functions presented by *Evans and Griffiths* [1974], may be employed to extract such weak signals from the impulsive ELF noise environment. Although the generated ELF signals were successfully detected using entirely linear analysis methods in this work, such nonlinear data extraction methods may aid in the reduction of uncertainty in the final radiated power estimates.

[27] The lack of multiple modulation frequencies usable for definitive polarization measurements during this experiment impedes our ability to further limit the range of ionospheric electron density profiles and thereby the range of ELF power radiated. Future experiments may choose to take advantage of the observation by *Barr et al.* [1988] that pointing the HF beam in the general direction of the receiver increases the observed SNR at the receiver, although we did not take advantage of this fact. Furthermore, future experiments are likely to have more success evaluating ionospheric conditions as well as ELF source parameters using receivers located closer to the ELF source region than ~4400 km.

[28] **Acknowledgments.** This work was supported by the High frequency Active Auroral Research Program (HAARP), the Air Force Research Laboratory (AFRL), the Defense Advanced Research Programs Agency (DARPA), and the Office of Naval Research (ONR) via ONR grants N00014-00-1-0643, N00014-05-C-0308, and N00014-03-1-0630 to Stanford University.

[29] Amitava Bhattacharjee thanks Vikas Sonwalkar and another reviewer for their assistance in evaluating this paper.

References

- Balanis, C. A. (1982), *Antenna Theory: Analysis and Design*, 805 pp., HarperCollins, New York.
- Barr, R. (1998), The generation of ELF and VLF radio waves in the ionosphere using powerful HF transmitters, *Adv. Space Res.*, *21*, 677–687.
- Barr, R., and P. Stubbe (1991), ELF radiation from the Tromsø “super heater” facility, *Geophys. Res. Lett.*, *18*, 1035–1038.
- Barr, R., M. T. Rietveld, H. Kopka, P. Stubbe, and E. Nielsen (1985), Extra-low-frequency radiation from the polar electrojet antenna, *Nature*, *317*, 155–157.
- Barr, R., P. Stubbe, M. T. Rietveld, and H. Kopka (1986), ELF and VLF signals radiated by the “polar electrojet antenna”: Experimental results, *J. Geophys. Res.*, *91*, 4451–4459.
- Barr, R., M. T. Rietveld, P. Stubbe, and H. Kopka (1988), Ionospheric heater beam scanning: A realistic model of this mobile source of ELF/VLF radiation, *Radio Sci.*, *23*, 1073–1083.
- Barr, R., P. Stubbe, and H. Kopka (1991), Long-range detection of VLF radiation produced by heating the auroral electrojet, *Radio Sci.*, *26*, 871–879.
- Demirkol, M. K., U. S. Inan, T. F. Bell, S. G. Kanekal, and D. C. Wilkinson (1999), Ionospheric effects of relativistic electron enhancement events, *Geophys. Res. Lett.*, *26*, 3557–3560.
- Evans, J. E., and A. S. Griffiths (1974), Design of a sanguine noise processor based upon world-wide extremely low frequency (ELF) recordings, *IEEE Trans. Commun.*, *22*(4), 528–539.
- Ferguson, J. A., and F. P. Snyder (1987), The segmented waveguide programs for long wavelength propagation calculations, *Tech. Doc. Nav. Ocean Syst. Cent. U. S.*, 1071.
- Ferraro, A. J., H. S. Lee, R. Allshouse, K. Carroll, A. A. Tomko, F. J. Kelly, and R. G. Joiner (1982), VLF/ELF radiation from the ionospheric dynamo current system modulated by powerful HF signals, *J. Atmos. Terr. Phys.*, *44*, 1113–1122.
- Getmantsev, C. G., N. A. Zuikov, D. S. Kotik, L. F. Mironenko, N. A. Mityakov, V. O. Rapoport, Y. A. Sazonov, V. Y. Trakhtengerts, and V. Y. Eidman (1974), Combination frequencies in the interaction between high-power short-wave radiation and ionospheric plasma, *Sov. Phys. JETP, Engl. Transl.*, *20*, 101–102.
- James, H. G. (1985), The ELF spectrum of artificially modulated *D/E*-region conductivity, *J. Atmos. Terr. Phys.*, *47*, 1129–1142.
- Kimura, I., A. Wong, B. Chouinard, T. Okuda, M. McCarrick, I. Nagano, K. Hushimoto, R. Wuerker, M. Yamamoto, and K. Ishida (1991), Satellite and ground observations of HIPAS VLF modulation, *Geophys. Res. Lett.*, *18*, 309–312.
- Lev-Tov, S. J., U. S. Inan, and T. F. Bell (1995), Altitude profiles of localized *D* region density disturbances produced in lightning-induced electron precipitation events, *J. Geophys. Res.*, *100*, 21,375–21,384.
- Lunnen, R. J., H. S. Lee, A. J. Ferraro, T. W. Collins, and R. F. Woodman (1984), Detection of radiation from a heated and modulated equatorial electrojet current system, *Nature*, *311*, 134–135.
- Moore, R. C., C. P. Barrington-Leigh, U. S. Inan, and T. F. Bell (2003), Early/fast VLF events produced by electron density changes associated with sprite halos, *J. Geophys. Res.*, *108*(A10), 1363, doi:10.1029/2002JA009816.
- Moore, R. C., U. S. Inan, and T. F. Bell (2006), Observations of amplitude saturation in ELF/VLF wave generation by modulated HF heating of the auroral electrojet, *Geophys. Res. Lett.*, *33*, L12106, doi:10.1029/2006GL025934.
- Papadopoulos, K., T. Wallace, G. M. Milikh, W. Peter, and M. McCarrick (2005), The magnetic response of the ionosphere to pulsed HF heating, *Geophys. Res. Lett.*, *32*, L13101, doi:10.1029/2005GL023185.
- Pappert, R. A., and D. G. Morfitt (1975), Theoretical and experimental sunrise mode conversion results at VLF, *Radio Sci.*, *10*, 537–546.
- Pappert, R. A., and F. P. Snyder (1972), Some results of a mode-conversion program for VLF, *Radio Sci.*, *7*, 913–923.
- Platino, M., U. S. Inan, T. F. Bell, M. Parrot, and E. J. Kennedy (2006), DEMETER observations of ELF waves injected with the HAARP HF transmitter, *Geophys. Res. Lett.*, *33*, L16101, doi:10.1029/2006GL026462.
- Stubbe, P., H. Kopka, M. T. Rietveld, and R. L. Dowden (1982), ELF and VLF generation by modulated HF heating of the current carrying lower ionosphere, *J. Atmos. Terr. Phys.*, *44*, 1123–1135.
- Vilaseñor, J., A. Y. Wong, B. Song, J. Pau, M. McCarrick, and D. Sentman (1996), Comparison of ELF/VLF generation modes in the ionosphere by the HIPAS heater array, *Radio Sci.*, *31*, 211–226.
- Wait, J. R., and K. P. Spies (1964), Characteristics of the Earth–ionosphere waveguide for VLF radio waves, *U. S. NBS Tech. Note*, 300.

T. F. Bell and U. S. Inan, Department of Electrical Engineering, Stanford University, 350 Serra Mall, Stanford, CA 94305, USA.

E. J. Kennedy, Information Technology Division, U.S. Naval Research Laboratory, Washington, DC 20375, USA.

R. C. Moore, Department of Electrical and Computer Engineering, 319 Benton Hall, University of Florida, P.O. Box 116200, Gainesville, FL 32611-6200, USA. (robert.moore@gmail.com)